NANO LETTERS

Letter

pubs.acs.org/NanoLett

Probing from Both Sides: Reshaping the Graphene Landscape via Face-to-Face Dual-Probe Microscopy

Franz R. Eder, Jani Kotakoski, Katharina Holzweber, Clemens Mangler, Viera Skakalova, and Jannik C. Meyer*

Department of Physics, University of Vienna, Boltzmanngasse 5, 1090 Vienna, Austria

Supporting Information

ABSTRACT: In two-dimensional samples, all atoms are at the surface and thereby exposed for probing and manipulation by physical or chemical means from both sides. Here, we show that we can access the same point on both surfaces of a few-layer graphene membrane simultaneously, using a dual-probe scanning tunneling microscopy (STM) setup. At the closest point, the two probes are separated only by the thickness of the graphene membrane. This allows us for the first time to directly measure the deformations induced by one STM probe on a free-standing membrane with an independent second probe. We reveal different regimes of stability of few-layer graphene and show how the STM probes can be used as tools to shape the membrane in a controlled manner. Our work opens new avenues for the study of mechanical and electronic properties of two-dimensional materials.

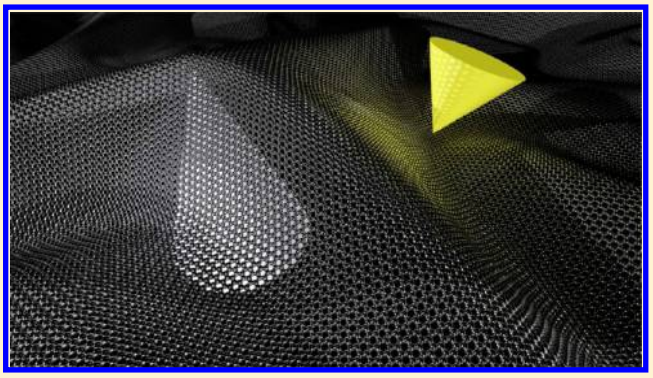

KEYWORDS: *Graphene, graphene membrane, scanning tunneling microscopy, multiprobe STM, mechanical deformation, molecular dynamics simulation*

Already two decades ago, individual atoms were manipulated with the scanning tunneling microscope in order to create novel structures and to explore the emerging quantum phenomena.[1,2] While the basic principles behind STM have not changed, recent developments integrating multiple probes within one device[3] have led to more flexibility in imaging and probing materials. Although the interprobe distances are already impressively short, the dimensions of the probes themselves pose an inherent limit for the achievable distance. Two-dimensional materials, such as graphene,[4] provide a unique way to circumvent this problem. On a free-standing membrane, the same position can be accessed from opposing sides, and in the case of a monolayer sample one might even put both probes on the same atom. However, this requires the ability to place the probes within each other's range of movement, as well as a sample that is stable enough to withstand simultaneous probing from both sides. Despite the intuitive appeal of this approach, to the best of our knowledge it has never been tried before.

Research into graphene, the ultimate 2D material, has already revealed surprises in the often disregarded third dimension. Instead of a simple lowland, this hexagonally structured carbon membrane has turned out to contain a rich landscape of hills and valleys when suspended,[5−9] and to partially follow the surface morphology when laying on a substrate.[10−15] However, recent STM experiments on free-standing graphene[9,16−19] indicate that tip-induced deformations of the graphene membrane are the predominant effect to the height profiles, meaning that the membrane follows the probe rather than vice versa.

The present study builds on the previous works that discussed the effect of out-of-plane deformations in suspended graphene induced by STM tips[9,16−19] and the gate voltage-driven switching between convex and concave forms.[19,20] We first demonstrate how an STM probe can impose a similar switch on few-layer graphene under appropriate conditions and in both directions. Then, we place another probe at the same position but on the other side of the sample. With varying conditions on the first (stationary) probe, the second (scanning) probe will observe one of two landscapes: either a small pointlike feature or a significantly larger mountain. These are identified in corroboration with atomistic simulations as two regimes where the initial deformations of the membrane are either maintained or stretched out. Finally, by displacing and retracting the second probe we demonstrate an accurate control over the local height of the membrane.

For our dual-probe STM experiments, we employed a custom-made device specifically designed for this study. In this device, two independent STM units are combined as shown in Figure 1a. Two scan heads, facing each other from opposing sides, are mechanically fixed to a support, which also holds the sample. A coarse alignment of the scan heads within the plane

Received: November 20, 2012
Revised: March 15, 2013

   dx.doi.org/10.1021/nl3042799 | *Nano Lett.* XXXX, XXX, XXX−XXX

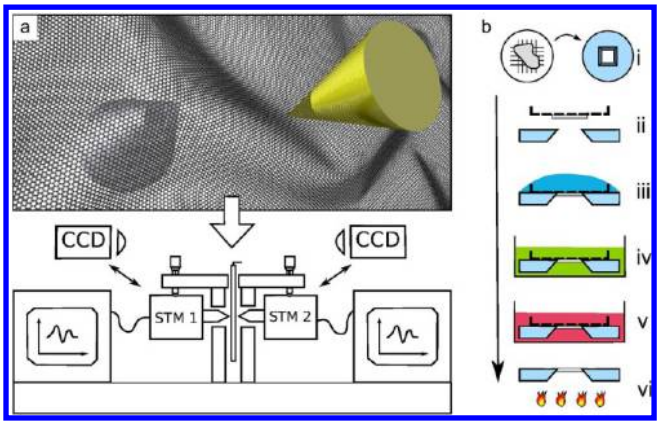

Figure 1. Experimental setup and sample preparation. (a) The 2× STM setup: Two standard STM units are mounted opposite to each other with a thin sample in the middle. Each scan unit can be replaced with a CCD camera to align the respective other tip. (b) Flowchart representation of graphene transfer from a grid to a gold-coated silicon substrate (i); (ii) alignment of the sample on top of the window; (iii) evaporation of a drop of isopropanol on top of the sample increases adhesion between the flake and the substrate; (iv) softening of the support foil of the grid (10 min in a chloroform bath); (v) dissolution of the foil in hot *N*-methyl-2-pyrrolidone bath (at 100 °C for 1 h) and rinse first in high purity acetone and then in isopropanol; (vi) heat treatment in vacuum (at 350 °C for 1 h).

normal to the probes is done with micrometer screws. To facilitate the alignment, each of the scan heads can be replaced by a charge-coupled device (CCD) camera. All experiments were carried out under ambient conditions. We prepared few-layer graphene membranes by mechanical exfoliation and subsequent transfer to grids as has been described previously.[21] We then transferred the membranes from the grids to gold-coated silicon substrates with a single window with sizes between 2 and 25 μm. The preparation process is outlined in Figure 1b and described in the Methods section. Our samples are free-standing few-layer graphene membranes (5−8 layers). Thinner membranes, in particular monolayers, were not stable in our STM, which we attribute to the ambient-conditions environment (comparing to earlier studies with similar sample geometry but using ultrahigh vacuum setups[9,17,19]).

We first show an experiment using a single tip, where a reversible transition between a convex and concave shape of the membrane is induced by adjusting the tunneling conditions. Importantly, this demonstrates that the STM tip can be used to both push and pull the membrane with a sufficient force to create permanent deformations. For this experiment, we used a suspended few-layer graphene sample with a perforated support foil (see Methods). The initial scan showed the membrane in a concave geometry, that is, hanging away from the probe inside the circular hole of the foil (see Figure 2a regime 1). We point out that the initial shape seems to be random since we observed both convex and concave structures in other experiments. In the beginning, our tunneling parameters were set to $U = -0.2$ V, $I = 1$ nA. We then started to increase the (negative) bias voltage in order to increase the force with which the tip pulls on the membrane (Figure 2b regime 1). The recorded line-profiles remained unchanged until $U = -1.2$ V. Then, an abrupt change occurred. The membrane which was initially hanging ∼10 nm below the edges of the foil transformed into a bulging structure ∼15 nm above (Figure 2a,b regime 2). This process is remarkably similar to the gate-voltage-driven snap-through event reported by Lindahl et al.[20] After the transformation, we changed the tunneling conditions by increasing the current and lowering the voltage to bring the probe close enough to the sample for Pauli repulsion to become the dominant interaction. Under these conditions we then started to transform the membrane back from convex to concave shape (Figure 2a,b regime 3). This reverse change takes place more gradually and requires a significantly (ca. 100×) smaller tunneling resistance, implying a high repulsive force.[22] In the example of Figure 2, the transition from regime 2 to 3 took place at $U = -0.01$ V, $I =$ 1 nA. Figure 2c shows schematic presentations of the proposed membrane configurations during scanning. The data in Figure 2

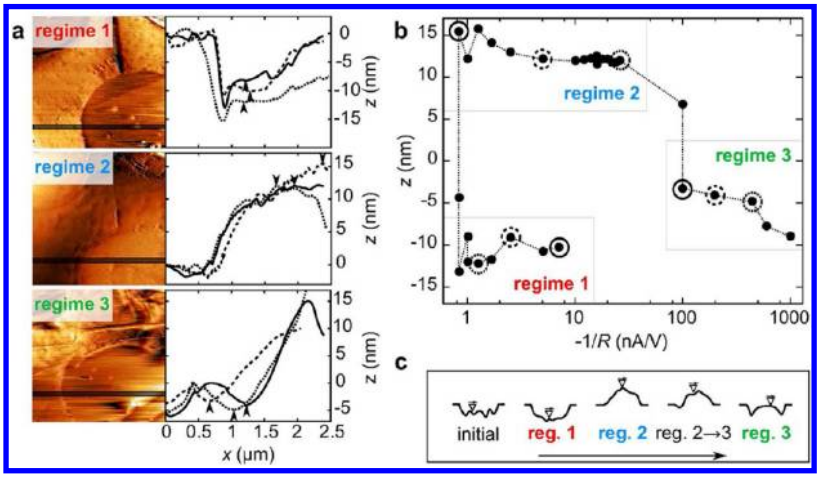

Figure 2. Tip-initiated snap-through process. (a) Example STM micrographs (scan size 2.5 μm) are presented for each of the three regimes (1−3) along with three example profiles measured from images along the marked line shown in the micrographs. The supported area is taken as reference ($z = 0$) and the membrane height is measured from $z = 0$ up (or down) to its peak position beyond the edge of the suspended part, as indicated by the arrows. The transition from concave to convex shape is abrupt (1→2), whereas the opposite transition (2→3) takes place gradually. (b) Height difference between the substrate and the highest or lowest point of the suspended membrane as a function of the inverse tunneling resistance. The points marked with circles correspond to the line profiles shown in panel a for each region. Line styles of the circles match those of the corresponding line profiles. (c) Schematic presentations of the proposed configurations of the membrane during scanning. The triangle represents the scanning tip.

dx.doi.org/10.1021/nl3042799 | *Nano Lett.* XXXX, XXX, XXX−XXX

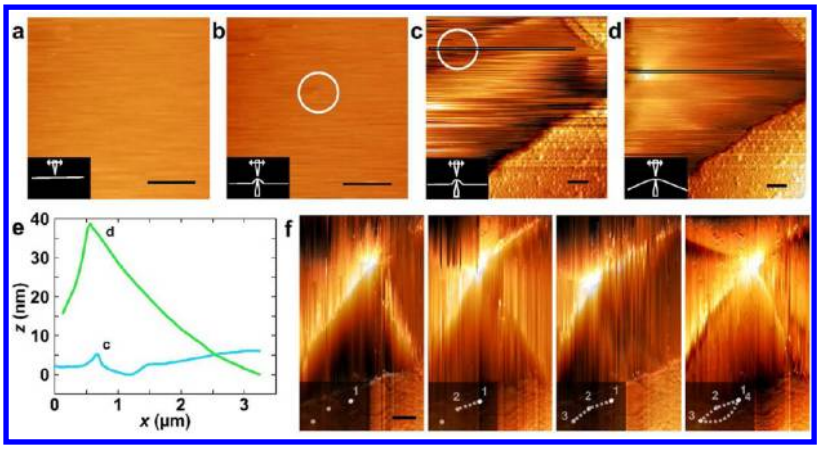

Figure 3. Effect of the second tip on recorded images. (a) STM micrograph of graphene as recorded with one tip only. (b) A small pointlike feature that appears as the second tip comes into contact with the opposite side of the membrane (position of the feature is indicated by the circle). (c) Another point feature (position indicated by the circle), which similarly appeared upon contact with the second tip and (d) transformation to the "mountain" regime by repeated scanning under fixed conditions. Insets in panels a–d are schematic drawings of the proposed configuration of the membrane under the influence of two tips. (e) Line scans indicating the size of the features in panels c and d along the marked lines. (f) A series of STM micrographs showing stepwise motion of the opposing (stationary) tip. The insets highlight the path tracked by the other tip (dotted line is for guiding the eye). Parameters for the stationary tip were (b) $U = -0.1$ V and $I = 3.3$ nA, (c,d) $U = -0.1$ V and $I = 4$ nA, (f) $U = -0.1$ V and $I = 3.5$ nA. Parameters for the scanning tip were (a–d): $U = -0.1$ V and $I = 0.5$ nA and (f) $U = -0.1$ V and $I = 1.1$ nA. All scale bars are 500 nm.

was measured in one continuous experiment (i.e., by continuously scanning while changing the tunneling bias and current after each frame), starting from regime 1 and ending at regime 3. The Supporting Information contains another similar experiment as well as a table with the tunneling conditions at each point of the transition.

After establishing conditions for manipulating the membrane, we introduce the second STM probe on the backside of the sample opposing the first one (see Methods). For these experiments (Figure 3), we used a slightly different sample geometry (having a rectangular instead of a circular suspended membrane, see Methods). After the alignment, the two probes are within each other's scanning range. In the first set of double-tip experiments, a constant current was maintained on the second (stationary) probe, which means that it applies an approximately constant force on the membrane. We observed two different regimes in the experiment. The first one is a small, localized point feature (Figure 3b,c, see also Supporting Information), which does not seem to affect the shape of the membrane further away from the stationary tip. The second regime is a larger mountain (Figure 3d,f), which extends all the way to the rim of the suspended membrane. As a surprising display of the mechanical strength of graphene, it is even possible to move the top of the mountain, which corresponds to the location of the opposite probe, in the lateral direction. In other words, we can directly observe the motion of one STM tip in subsequent images recorded on the other side of the membrane. During this experiment, both the quasi-stationary and the imaging probe were held at a constant current to maintain constant force between the tip and the sample. A series of four STM images from this experiment is shown in Figure 3f, where the summit of the mountain tracks a path following the movements of the probe as observed with the scanning tip. In order to make the movement clearly visible, the individual steps were more than 500 nm long. In this experiment the mountain appears as approximately 60 nm high in the topographic image.

Finally, after moving the stationary probe in the lateral direction we show that starting from the mountain shape we can also impose control over the contour of the membrane by adjusting the vertical position of this probe. We switched off the feedback loop of the probe, thereby defining a fixed height of the membrane at the position of the second tip (Figure 4a). We then recorded long image sequences (~100 images) while gradually pulling the probe away from the membrane. Correspondingly, the mountain top sinks, step-by-step, until a deep valley is formed (Figure 4a–d). This valley approximately mirrors the original mountain shape. After a full reversal of the mountain, when the force required to deform the membrane overcomes the adhesive force induced by the probe, the connection between membrane and probe breaks and the membrane snaps back to a freely suspended configuration. The total range of the deformation is more than 60 nm. Despite the large deformation caused by the stationary tip, the effect of the scanning tip can be seen in the contours presented in Figure 4f. In all scans between the initial mountain (Figure 4a) and the final valley configuration (Figure 4d), the line-profiles between the substrate and the stationary tip curve toward the scanning tip. The stationary tip also stabilizes the membrane. In the free-standing areas, the tip-induced deformations of the membrane lead to line-to-line variations during acquisition of the scanned image. These variations are absent on the supported area and in a small area around the stationary tip (Figure 4a–d). The complete deformation of this membrane is shown in Supporting Information video 1. For this deformation sequence, we also analyzed the strain of the membrane, by comparing the length of the profiles (Figure 4f, solid lines) for all deformed cases and the final length after detaching the second tip (Figure 4f, dashed line). Surprisingly, we find that this length remains constant with changes below 0.1% (see Supporting Information). This indicates that we are not significantly stretching the carbon bonds within the graphene membrane but rather changing the shape of existing deformations.

We now turn to the analysis and discussion of our experimental results. We carried out molecular dynamics (MD) simulations with a scaled down model of the suspended membrane, which provided qualitatively similar observations as

dx.doi.org/10.1021/nl3042799 | *Nano Lett.* XXXX, XXX, XXX–XXX

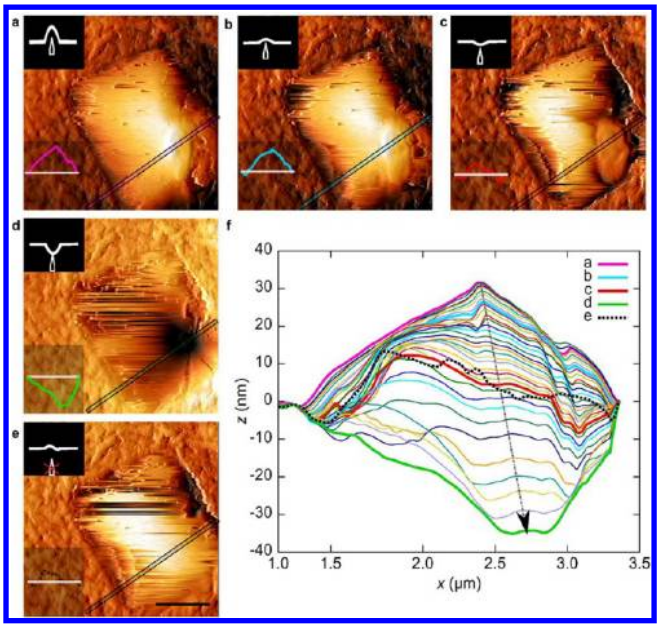

Figure 4. Controlling the contour of a graphene membrane. (a–d) Topography image sequence, recorded on one side of the membrane, showing the transformation of a mountain into a deep valley by gradually pulling the probe on the other side (constant height mode) away from the membrane while maintaining attraction. (e) Final configuration of the membrane after it snaps back to a freely suspended configuration. The pictograms in the upper left corner show the tip-membrane configurations. The line profiles in the lower left corner show the contour of the membrane along the line marked in the images. These contours are also contained in panel f. Scale bar is 1 μm. (f) Line-profiles of the complete data set. The nearly vertical, dash-dotted arrow highlights the position of the stationary tip. Line profiles were recorded in a sequence from top to bottom as indicated by the arrow, except for the black dotted line, which shows the membrane configuration after the second tip was fully retracted.

in the experiments. Generally, it is well-known that STM images can be affected by tip-induced elastic deformations of the sample.[23] In the case of free-standing membranes, such effects become even more important.[9,16−19] Therefore, it is necessary to understand the effect of the probe on the structure of the membrane at the atomic level. The rippled form of free-standing graphene at the nanometer length scale has been revealed by transmission electron microscopy (TEM)[5,7] and was recently observed with STM.[9,24] However, the impact of scanning on the structure of a free-standing membrane is difficult to interpret from the results obtained during such a scan.

In order to elucidate the effects of a moving STM tip on a free-standing graphene membrane, we used the following approach (see Methods for details). First, we created a ∼17 nm × 17 nm model of graphene under 2% compression and then simulated the evolution of the structure by MD simulations at a finite temperature (300 K) for 5 ps. Remarkably, this is sufficient to obtain a static, rippled structure as shown in Figure 5a. Figure 5a–f shows how the structure changes during the simulated scan. Corresponding line-profiles are presented in Figure 5g. Interestingly, the "measured" line profile ("probe trace" in Figure 5g) differs from any of the shapes assumed by the membrane before, during, or after the scan. Moreover, the amplitude of the "measured" ripples is significantly less than those in the actual structure. Comparing the contours of the membrane before and after the scan shows that the simple act of scanning can locally turn concave locations into convex ones and vice versa.

Next, we consider the transformation between a concave and convex form by the influence of the tip. We started again with a rippled graphene membrane, this time with fixed edges to model the substrate–graphene interaction at the rim of the suspended area, and applied gradually increasing force to one of the atoms in a direction normal to the plane of the membrane (see Supporting Information and Methods). The initial, rippled configuration happens to be mostly concave in this example and remained as such when forces below 0.05 eV/Å were applied. A force above 0.05 eV/Å was sufficient for this membrane to assume a convex configuration. After the convex geometry had formed, similar to the experiments, we tried to push it back by applying a force in the opposite direction. However, this shape now remained stable up to 50 eV/Å after which increasing the force resulted in breaking of bonds. Only by simulating several subsequent full scans over the membrane were we able to lower the convex membrane back into a concave configuration. The entire deformation process is shown in Supporting Information video 2. The overall conclusion from the experiments and simulations is as follows. The as-prepared membrane contains initial, presumably random, out-of-plane deformations that are in-between the fully concave or convex shapes. For this configuration, a low force is sufficient to stretch out the deformations and obtain the energetically more favorable stretched-out structure (up or

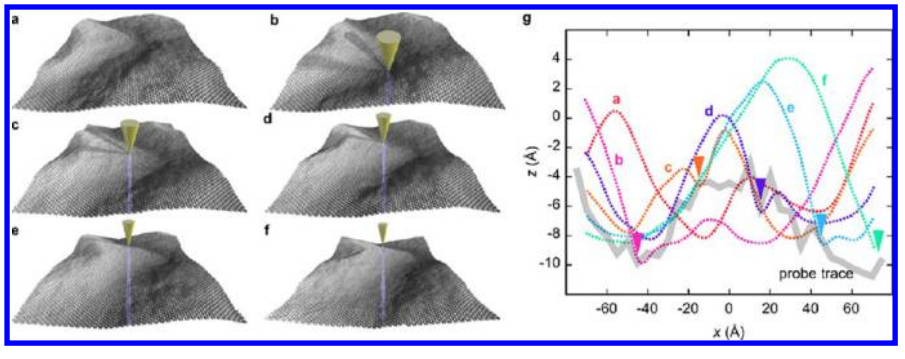

Figure 5. Effect of scanning on a free-standing graphene membrane. (a–f) Atomic structure of the membrane during the scan along a single scan line (the cone represents a force applied to the atoms directly underneath). (g) Line profiles of the structures presented in panels (a–f) (dotted, colored lines). Filled triangles mark the positions of the probe for each curve. The simulated probe trace is shown as a gray line; it clearly differs from all of the actual membrane configurations. The size of the modeled membrane is ∼17 nm × 17 nm.

dx.doi.org/10.1021/nl3042799 | *Nano Lett.* XXXX, XXX, XXX−XXX

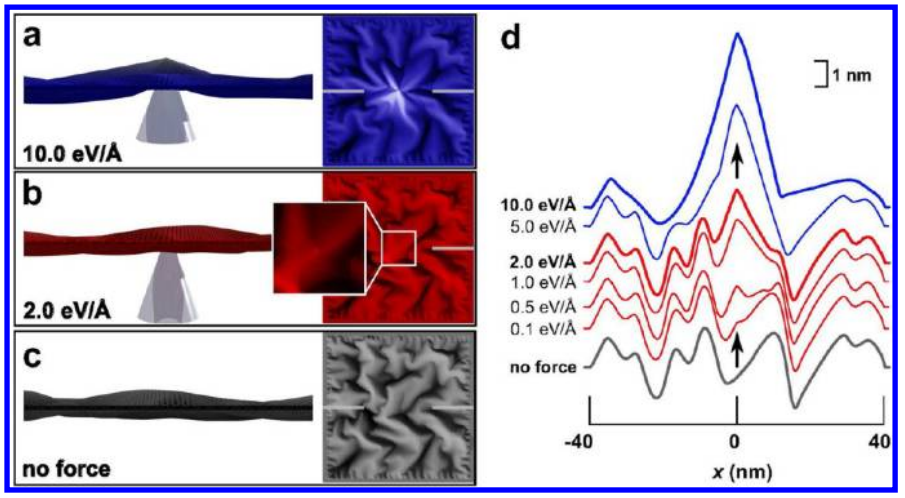

Figure 6. Simulated transformations for point and mountain features. (a–c) Side (left) and top views (right) of a model structure when three different total upward forces (from bottom to top: no force, 2.0 eV/Å, 10.0 eV/Å) are applied in the central part. The field of view in the top views is 84 nm × 84 nm (complete simulated area), while the side views show a central section of ca. 40 nm. (d) Line profiles for the same model structure along the white markers in the top views of panels a–c under forces between 0–10.0 eV/Å. At lower forces (red), a local pointlike feature is apparent in the profiles (see also inset in b) with no further changes in the membrane shape, whereas higher forces result in stretching out the ripples in the vicinity of the applied force and thus in significantly larger deformations. The arrows show the location and direction of the applied force.

down, depending on the direction of force applied in the first experiment). After this, pushing or pulling the membrane to the opposite side requires imposing strain to the material that requires a significantly higher force.

Finally, we aimed at understanding the two distinct regimes, the "point" and the "mountain" feature as observed by the double tip STM. Our initial hypothesis was that the two regimes correspond to situations where the force imposed by the stationary tip is either lower (point) or higher (mountain) than what is required to stretch out the ripples of the membrane, which formed during the sample preparation. To test this hypothesis, we created six examples of somewhat larger models (84 nm × 84 nm) with locally different ripple structures (see Methods). We then applied varying forces to 10 atoms in the middle of the membrane and monitored the change in the shape of the membrane. Three examples of the resulting structures for one of the samples are presented in Figure 6a–c. The corresponding line profiles, along with profiles for intermediate forces, are presented in Figure 6d. As can be seen in the images, we observe two kinds of deformations depending on the applied force. At lower forces, the modeled tip induces a clear change in the line profile, limited from both sides by the initial ripples of the membrane. At higher forces, the ripples stretch out and a clearly larger deformation appears. These two cases correspond directly to the experimentally observed regimes, confirming our hypothesis. Although both regimes were observed for all six studied structures, the forces required for the transformations varied by more than an order of magnitude (from 1 to 20 eV/Å) depending on the initial structure. Hence, the deformation depends on the balance between the imposed force (and thus selected tunnelling conditions), and the initial structure of the membrane. Remarkably, when the force is close to the deformation threshold, the effect of continuous scanning (by modifying the structure of the sample as demonstrated in Figure 5) can trigger a transition between these two cases, as was experimentally observed in Figure 3c,d, which shows this transition between two subsequent scans at the same conditions. We point out that stretching out the ripples during the simulated transformations requires forces that are approximately an order of magnitude lower (even for the highest ones) than what would be required to deflect a similarly sized nonrippled graphene membrane without prestrain to a similar extent according to a continuum mechanics model.[25] Hence, also in our simulated experiment, no significant straining of the membrane (stretching of bonds) occurs. We can thus conclude that the out-of-plane deformations are reshaped by interaction with the STM tip, but they remain within the degree of freedom given by the initial slack or compression of the membrane.

In summary, we have shown that two-dimensional materials can be probed simultaneously from both sides and at the same location. Using a face-to-face dual probe STM setup, we have for the first time directly measured the tip-induced deformations by an independent second probe. We have shown that an STM tip modifies the graphene landscape during each scan and can induce permanent changes in the shape by both attractive and repulsive tip–sample interaction. This provides means for controlling graphene morphology beyond substrate variation. Moreover, we have clarified the response of the membrane under the external forces of the tip by taking into account initial random out-of-plane deformations of the membrane. Finally, we demonstrate an accurate control of local curvature and height of the membrane, which leads to new possibilities toward deformation engineering of graphene.[26] Overall, our experiments open hitherto unexplored avenues for the study of 2D materials. The unobstructed combination of two local probes adds additional dimensions to the versatility of STM, which can likely be extended from probing mechanical properties and local deformations (as shown here) to include, for example, electronic effects under deformation,[13,19] local manipulation of defects, ad-atoms[27–29] or molecules[1,30] on both sides of the membrane, or the study of quantum interference effects[2] with multiple probes. Further perspectives arise with the use of other types of probes, which may, for example, induce and sense forces[25,31,32] or near-field optical signals[33,34] instead of tunneling currents. In principle, any mode of operation of any scanning probe instrument may conceivably be combined with each other in a similar dual-probe setup,

dx.doi.org/10.1021/nl3042799 | Nano Lett. XXXX, XXX, XXX–XXX

which opens a larger number of new routes for exploring the physics and material properties of ultrathin membranes.

Methods. *Double-Tip Experiments.* The 2× STM setup presented in Figure 1a was built specifically for this study by DME, Danish Micro Engineering A/S, Herlev, Denmark. It consists of two standard DME's STM scanners mounted on a custom base that holds the scanners on opposing sides of the sample. This base was designed so that each scanner and the sample can be removed and replaced with a position accuracy of a few (less than five) micrometers, and a CCD microscope camera can be placed into the position of each scanner. Each scan head is connected to one Dual Scope C-26 controller (DME). They were controlled by two instances of software DME-Scantool. In order to reach the same alignment for both of the scan heads, the following procedure was used: (1) The sample holder is placed in a solid support ("guide") in between the two scanners. (2) CCD camera is attached to one side of the guide and adjusted to have the sample area in the field of view. The exact position of the graphene membrane is marked with a cross hair on a monitor. (3) The sample is removed from the guide and the first scan head (STM 1) is placed opposite to the camera and the probe is aligned with micrometer screws to match with the cross hair (in the focal plane of the camera). (4) The scan head is removed, and the sample is remounted. The camera is moved to the other side. (5) Steps 1 and 2 are repeated for the second scan head (STM 2). (6) Finally, the camera is removed and both scanners are attached. The tip of one scanner is now within the scan range (5 μm) of the other scanner, and the exact alignment of the tips is possible by using the piezos since the tip-induced deformation of the membrane by one stationary tip is visible in the scanned image of the other tip.

Sample Preparation. Our sample preparation follows well-known procedures for the transfer of graphene sheets from silicon/silicon dioxide to a target substrate by using a dissolvable plastic film as an intermediate carrier. In our case, we first transfer the mechanically exfoliated few-layer graphene sheets to plastic-only Quantifoil transmission electron microscopy (TEM) grids with 1.2 μm sized holes. This "perforated" plastic film has the added advantage that those graphene areas that coincide with holes are never in contact with the polymer. Because these grids are nonconductive and not rigid enough for STM experiments, we then transferred the samples to 2.65 mm × 2.65 mm × 200 μm silicon window frames purchased from Silson Ltd., U.K. Those chips, originally intended for TEM use, have a single rectangular window at the center with sizes ranging from ~2 to 25 μm, from which we selected the smaller ones. To ensure conductivity, we coated the silicon frames with a thin gold layer prior to the transfer. In the single-tip experiment presented in Figure 2, we did not dissolve the plastic film (stopping the process at step iii in Figure 1b) and thereby obtained graphene membranes on a circular support. In other experiments, the plastic film was dissolved in chloroform followed by methylpyrrolidone (heated to 100 °C), leaving the few-layer graphene suspended on the rectangular hole of the silicon window. Our STM tips were fabricated by a dynamical electrochemical etching method.[35] We used 0.35 mm polycrystalline tungsten wire and a 2 M KOH solution as the electrolyte. TEM images of an as-prepared STM tip are shown in the Supporting Information. The thickness of the graphene samples used in these experiments was between 5 and 8 layers and was determined optically.[36]

Simulations. The graphene structures used in the atomistic simulations consisted of either 11040 carbon atoms (17 nm × 17 nm; Figure 5, Supporting Information Figure S1) or 276 800 atoms (84 nm × 84 nm; Figure 6). To mimic the experimental conditions, we initially put the structures under 2% compression and then carried out molecular dynamics simulation at a finite temperature (300 K) for 5 ps. After this step, we obtain a rippled structure as shown in Figures 5a or 6c. The carbon−carbon interaction was modeled using the reactive bond-order potential by Brenner et al.,[37] and the temperature of the system was maintained according to the scheme of Berendsen et al.[38] All simulated structures were periodic in the in-plane directions of graphene. For simulations presented in Figure 5, all of the atoms were allowed to move, whereas for those presented in Figure 6 and Supporting Information Figure S1 the outermost atoms (atoms within 1nm from the boundary) were fixed to model the edge of the substrate.

In the scan simulation presented in Figure 5, the effect of the scanning probe was modeled by applying a force of 1 eV/Å on those atoms exactly under the tip (assuming a tip diameter of 3 Å). The tip was moved from $y = -75$ Å to $y = 75$ Å with a step size of 5 Å. For each of the tip positions, the atomic structure was optimized with conjugate gradient energy minimization scheme while maintaining the force on the atoms under the tip. Then, a 20 ps molecular dynamics simulation at 300 K was carried out before moving the tip further.

In the simulations presented in Supporting Information Figure S1 and supplementary video 2, we first applied an increasing (upward) force on one of the atoms in the middle of the graphene sheet until the structure optimization resulted in a convex shape for the optimized structure instead of a concave shape which was obtained with no force. Then, an increasing opposite force was applied to the same atom in the convex structure until the force was high enough to break the membrane. After this, we modeled the effect of scanning on the membrane, as described above, by moving the tip gradually over the whole sample area and applying a downward force on the atoms under the tip. As previously, the force was applied to 10 atoms under the tip, which prevented the membrane from breaking even when the total force was increased. The resulting decrease of the height of the membrane after four subsequent scans is presented in the Supporting Information.

To obtain structures with locally different ripple configurations used to study the point and mountain features (Figure 6), we ran extended MD simulations at a high temperature (2500 K) for a total of 31 ps, which allowed the local ripple structure of the membrane to evolve without creating defects in the lattice. During this simulation, we saved six intermediate structures. Next, the effect of the stationary tip was again modeled by applying different static out-of-plane forces (between 0.1 and 20.0 eV/Å) to 10 atoms in the middle of each of the structures to study the local changes to the shape of the membrane as a function of the applied force.

We point out that our model system is a simplification of the experimental setup, since both the membrane size and thickness are scaled down in order to make simulations computationally feasible. However, our models capture the most important aspects of the experimental situation in a manner that provides a reasonably good qualitative understanding.

dx.doi.org/10.1021/nl3042799 | *Nano Lett.* XXXX, XXX, XXX−XXX

■ ASSOCIATED CONTENT

Supporting Information

Additional experimental STM data, additional simulations, TEM images of our STM tip, and the strain analysis of the deformed membrane. Supplementary video S1 shows the transformation of a tip-induced mountain to a valley by retracting the stationary tip of the double-tip STM, as shown in Figure 4 of the article. Supplementary video S2 shows the simulated deformations of a graphene membrane as described in the article. First, the membrane is pulled from a rough initial configuration into a convex shape by a force applied at the center. Then, repeated scanning with repulsive force from the tip pushes it back to a concave shape. This material is available free of charge via the Internet at http://pubs.acs.org.

■ AUTHOR INFORMATION

Corresponding Author

*E-mail: jannik.meyer@univie.ac.at.

Author Contributions

F.E. and J.K. carried out STM experiments, prepared samples, and analyzed the data. J.K. carried out atomistic simulations. K.H. contributed to experiments in Figure 2. C.M. and V.S. contributed to sample preparation and characterization. J.M. conceived and supervised the study. F.E., J.K., and J.M. wrote the paper.

Notes

The authors declare no competing financial interest.

■ ACKNOWLEDGMENTS

J.K. acknowledges computational resources from the Vienna Scientific Cluster and funding from the Austrian Science Fund (FWF): M 1481-N20.

■ REFERENCES

(1) Eigler, D.; Schweizer, E. *Nature* **1990**, *344*, 524−526.
(2) Crommie, M. F.; Lutz, C. P.; Eigler, D. M. *Science* **1993**, *262*, 218−20.
(3) Nakayama, T.; Kubo, O.; Shingaya, Y.; Higuchi, S.; Hasegawa, T.; Jiang, C. S.; Okuda, T.; Kuwahara, Y.; Takami, K.; Aono, M. *Adv. Mater.* **2012**, *24*, 1675−92.
(4) Geim, A. K.; Novoselov, K. S. *Nat. Mater.* **2007**, *6*, 183−91.
(5) Meyer, J. C.; Geim, A. K.; Katsnelson, M. I.; Novoselov, K. S.; Booth, T. J.; Roth, S. *Nature* **2007**, *446*, 60−3.
(6) Fasolino, a.; Los, J. H.; Katsnelson, M. I. *Nat. Mater.* **2007**, *6*, 858−61.
(7) Meyer, J. C.; Geim, A. K.; Katsnelson, M. I.; Novoselov, K. S.; Obergfell, D.; Roth, S.; Girit, C.; Zettl, A. *Solid State Commun.* **2007**, *143*, 101−109.
(8) Bangert, U.; Gass, M. H.; Bleloch, a. L.; Nair, R. R.; Geim, a. K. *Phys. Status Solidi A* **2009**, *206*, 1117−1122.
(9) Zan, R.; Muryn, C.; Bangert, U.; Mattocks, P.; Wincott, P.; Vaughan, D.; Li, X.; Colombo, L.; Ruoff, R. S.; Hamilton, B.; Novoselov, K. S. *Nanoscale* **2012**, *4*, 3065−3068.
(10) Geringer, V.; Liebmann, M.; Echtermeyer, T.; Runte, S.; Schmidt, M.; Rückamp, R.; Lemme, M.; Morgenstern, M. *Phys. Rev. Lett.* **2009**, *102*, 076102.
(11) Zhang, Y.; Brar, V. W.; Girit, C.; Zettl, A.; Crommie, M. F. *Nat. Phys.* **2009**, *5*, 722−726.
(12) Li, T.; Zhang, Z. *Nanoscale Res. Lett.* **2010**, *5*, 169−173.
(13) Levy, N.; Burke, S. a.; Meaker, K. L.; Panlasigui, M.; Zettl, A.; Guinea, F.; Castro Neto, a. H.; Crommie, M. F. *Science (New York)* **2010**, *329*, 544−7.
(14) Li, T.; Zhang, Z. *J. Phys. D: Appl. Phys.* **2010**, *43*, 075303.
(15) Scharfenberg, S.; Rocklin, D. Z.; Chialvo, C.; Weaver, R. L.; Goldbart, P. M.; Mason, N. *Appl. Phys. Lett.* **2011**, *98*, 091908.
(16) Mashoff, T.; Pratzer, M.; Geringer, V.; Echtermeyer, T. J.; Lemme, M. C.; Liebmann, M.; Morgenstern, M. *Nano Lett.* **2010**, *10*, 461−5.
(17) Xu, P.; Yang, Y.; Barber, S.; Ackerman, M.; Schoelz, J.; Qi, D.; Kornev, I.; Dong, L.; Bellaiche, L.; Barraza-Lopez, S.; Thibado, P. *Phys. Rev. B.* **2012**, *85*, 121406.
(18) Xu, P.; Yang, Y.; Barber, S.; Schoelz, J.; Qi, D.; Ackerman, M.; Bellaiche, L.; Thibado, P. *Carbon* **2012**, *50*, 4633−4639.
(19) Klimov, N.; Jung, S.; Zhu, S.; Li, T.; Wright, C. A.; Solares, S. D.; Newell, D. B.; Zhitenev, N. B.; Stroscio, J. A. *Science* **2012**, *336*, 1557−1561.
(20) Lindahl, N.; Midtvedt, D.; Svensson, J.; Nerushev, O.; Lindvall, N.; Isacsson, A.; Campbell, E. E. B. *Nano Lett.* **2012**, *12*, 3526−31.
(21) Meyer, J. C.; Girit, C. O.; Crommie, M. F.; Zettl, A. *Appl. Phys. Lett.* **2008**, *92*, 123110.
(22) Yamada, H.; Fujii, T.; Nakayama, K. *J. Vac. Sci. Technol., A* **1988**, *6*, 293.
(23) Soler, J.; Baro, A.; Garcia, N.; Rohrer, H. *Phys. Rev. Lett.* **1986**, *57*, 444−447.
(24) Tapaszto, L.; Dumitrica, T.; Kim, S. J.; Nemes-Incze, P.; Hwang, C.; Biro, L. P. *Nat. Phys.* **2012**, *8*, 739−742.
(25) Lee, C.; Wei, X.; Kysar, J. W.; Hone, J. *Science* **2008**, *321*, 385−8.
(26) Pereira, V.; Castro Neto, A. *Phys. Rev. Lett.* **2009**, *103*, 046801.
(27) Sessi, P.; Guest, J. R.; Bode, M.; Guisinger, N. P. *Nano Lett.* **2009**, *9*, 4343−7.
(28) Balog, R.; et al. *Nat. Mater* **2010**, *9*, 315−9.
(29) Wang, Y.; Brar, V. W.; Shytov, A. V.; Wu, Q.; Regan, W.; Tsai, H.-Z.; Zettl, A.; Levitov, L. S.; Crommie, M. F. *Nat. Phys.* **2012**, *8*, 653−657.
(30) Hamalainen, S. K.; Stepanova, M.; Drost, R.; Liljeroth, P.; Lahtinen, J.; Sainio, J. *J. Phys. Chem. C* **2012**, *116*, 20433−20437.
(31) Binnig, G.; Quate, C.; Gerber, C. *Phys. Rev. Lett.* **1986**, *56*, 930−933.
(32) Giessibl, F. J. *Appl. Phys. Lett.* **2000**, *76*, 1470.
(33) Hecht, B.; Sick, B.; Wild, U. P.; Deckert, V.; Zenobi, R.; Martin, O. J. F.; Pohl, D. W. *J. Chem. Phys.* **2000**, *112*, 7761.
(34) Hartschuh, A. *Angew. Chem., Int. Ed.* **2008**, *47*, 8178−91.
(35) Kazinczi, R.; Szocs, E.; Kalman, E.; Nagy, P. *Appl. Phys. A* **1998**, *66*, 535−538.
(36) Ni, Z. H.; Wang, H. M.; Kasim, J.; Fan, H. M.; Yu, T.; Wu, Y. H.; Feng, Y. P.; Shen, Z. X. *Nano Lett.* **2007**, *7*, 2758−63.
(37) Brenner, D. W.; Shenderova, O.; Harrison, J.; Stuart, S. J.; Ni, B.; Sinnott, S. B. *J. Phys.: Condens. Mat* **2002**, *14*, 783−802.
(38) Berendsen, H. J. C.; Postma, J. P. M.; van Gunsteren, W. F.; DiNola, A.; Haak, J. R. *J. Chem. Phys.* **1984**, *81*, 3684.